
THERMOELECTRIC PROPERTIES OF n - $\text{Bi}_2\text{Te}_{3-x}\text{Se}_x$ -In ($x = 0.15$ and 0.3) CRYSTALS



T.E. Svechnikova



M.A. Korzhuev

*(A.A. Baikov Institute of Metallurgy and Material
Science RAS, Laboratory of Semiconductor
Materials, Leninsky Ave., 49,
Moscow, 119991, Russia)*

- The Czochralski technique with liquid phase replenishment was used to prepare single crystals of n - $\text{Bi}_2\text{Te}_{3-x}\text{Se}_x$ -In ($x = 0.15$ and 0.3) solid solutions doped with $y = 0.1 - 2.0$ mol.% In_2Te_3 and small dopants of SbI_3 (up to 0.17 at.%) I, with the optimal current carrier concentration for the temperature range of $T = 300 - 400$ K ($n = 1.5 - 2.10^{19}$ cm $^{-3}$). As y increased from zero to $0.1 - 0.2$ mol.% In_2Te_3 , the thermoelectric figure of merit Z of alloys increased from $0.0029 - 0.003$ to $0.0031 - 0.0032$ 1/K and Z_{\max} position shifted by $\Delta T = 10 - 30$ K towards high temperatures ($(ZT)_{\max} = 0.87 \rightarrow -1.2$ for $y = 0.2$ mol.% In_2Te_3 at $T = 400$ K). With further increase in y from 0.2 to 2 mol.% In_2Te_3 , Z_{\max} value of alloys drastically decreased to 0.002 1/K, and Z_{\max} position shifted towards low temperatures. In this work, the observed effect is attributed to a change in electron mobility μ_n in the alloys on introduction of indium with allowance for a reduced amount of SbI_3 dopant introduced into solid solution in the course of optimization of electron concentration in the samples.

Introduction

Semiconductor alloys based on n - and p -type bismuth and antimony chalcogenides possess high thermoelectric figure of merit

$$Z = \alpha^2 \sigma / \kappa, \quad (1)$$

reaching its maximum Z_{\max} value $\sim 0.0028 - 0.003$ 1/K at close to room temperature (here α , σ and κ are thermoEMF, the electrical and thermal conductivity, respectively). Bismuth and antimony chalcogenides are widely used in various thermoelectric power converters (TPC), namely generators (TEG), coolers (TEC) and heaters (TEH) working close to room temperature [1]. In recent times, more interest is being shown in bismuth and antimony chalcogenides owing to development of processes for heat recovery from low-grade power sources where operating temperature is 100 – 200 K higher than room temperature [2]. Using bismuth and antimony chalcogenides in the corresponding devices requires their efficiency increase and a shift of Z_{\max} position towards high temperatures [3, 4].

For the nondegenerate case and one sort of current carriers, Z_{\max} value of thermoelectric materials is given by the expression

$$Z_{\max} \sim N m^{*3/2} (\mu / \kappa_L) T^{3/2} e^{r+1/2}, \quad (2)$$

where N is the number of electron (hole) ellipsoids in quasi-impulse space, $\mu = e\langle\tau\rangle/m_c$ is mobility of electrons (holes), m^* and m_c are the effective masses of density of states and conductivity, $\langle\tau\rangle$ is the average relaxation time of current carriers, κ_L is crystal lattice thermal conductivity, T is absolute temperature, r is scattering parameter, e is elementary charge [1, 4]. Z_{\max} position on the temperature scale is determined by the onset of alloy transition to intrinsic conduction and can be found from the relation

$$(E_g + E_F) \sim A k_B T_{\max}, \quad (3)$$

where E_g is the energy gap width, E_F is the Fermi energy of electrons (holes) counted from the band edge, k_B is the Boltzmann constant, T_{\max} is temperature corresponding to Z_{\max} position, A is coefficient depending on the band structure of semiconductor and the ratio between partial conductivities of electrons and holes $B = \sigma_n / \sigma_p$ in the samples ($A = 6 - 8$ for bismuth and antimony chalcogenides) [4]. From relations (2) and (3) it follows that, all other conditions being equal, Z_{\max} value of alloys will increase with the growth of μ/κ_L ratio, and T_{\max} value will increase with the growth of E_g and E_F . T_{\max} growth is also due to increase (for n -type samples) or decrease (for p -type samples) in parameter B that determines the onset of intrinsic conduction in the samples.

Relations (2) and (3) are widely used in the optimization of thermoelectric characteristics of bismuth and antimony chalcogenides by formation of solid solutions on their basis [5–7]. The basic mechanisms of Z growth in solid solutions include increase in μ/κ_L ratio and T_{\max} value [1]. According to relation (3), at $A = \text{const}$, T_{\max} of samples can be increased in two ways (Fig. 1). It is increase in the energy gap width E_g ($E_F - \text{const}$) ($1 \rightarrow 2 \rightarrow 3$) and (or) increase in the Fermi energy of samples E_F ($E_g - \text{const}$) ($3 \rightarrow 4 \rightarrow 5$, Fig. 1). The latter method is extensively employed in practice [1], despite considerable Z_{\max} decrease with the growth of E_F which is due to increased Fermi degeneracy of current carriers in the samples ($3 \rightarrow 4 \rightarrow 5$, Fig. 1) [1].

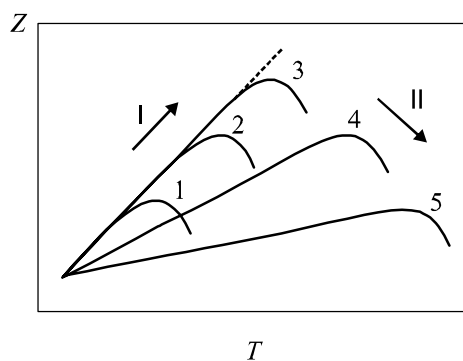


Fig. 1. Pattern of change in $Z = f(T)$ curves of thermoelectric materials with a shift of T_{\max} towards higher temperatures with increase in E_g (I \rightarrow 2 \rightarrow 3) ($E_F - \text{const}$) (I) and E_F (3 \rightarrow 4 \rightarrow 5) ($E_g - \text{const}$) (II). $E_g^1 < E_g^2 < E_g^3$; $E_F^3 < E_F^4 < E_F^5$.

On formation of solid solutions in $(\text{Bi}_2\text{Te}_3)_{1-x}(\text{Bi}_2\text{Se}_3)_x$ system, with the growth of $x = 0 \rightarrow 1$ the energy gap width of alloys is increased from $E_g = 0.16$ eV for Bi_2Te_3 to $E_g = 0.175$ eV for Bi_2Se_3 [8]. In so doing, current carrier mobility μ and lattice thermal conductivity κ_L decrease, the latter somewhat quicker [1]. As a result, for alloys of optimal compositions n - $\text{Bi}_2\text{Te}_{3-x}\text{Se}_x$ ($x = 0.15$ and 0.3) the maximum μ_n/κ_L ratio was observed, attended with the growth of $Z_{\max} = 0.0026 \rightarrow 0.0028 - 0.003$ 1/K and $T_{\max} = 230 \rightarrow 300$ K [1, 6, 7]. The presented Z_{\max} values $0.0028 - 0.003$ 1/K correspond to alloys additionally doped with a small amount of donor dopant $\langle \text{SbI}_3 \rangle$ (up to ~ 0.17 at.%) I, necessary for increase of electron concentration in material to the optimal value [1].

The objective of this work was to study the possibility of further increase in Z_{\max} and T_{\max} of n - $\text{Bi}_2\text{Te}_{3-x}\text{Se}_x$ -In ($x = 0.15$ and 0.3) alloys by additional doping solid solution with indium. For this purpose, from 0 to 2 mol.% of In_2Te_3 compound ($E_g = 1.07$ eV) was additionally introduced into n - $(\text{Bi}_2\text{Te}_{3-x}\text{Se}_x)$ -In ($x = 0.15$ and 0.3) alloys. Earlier it had been established that Bi_2Te_3 forms with In_2Te_3 the limited solid solutions $(\text{Bi}_2\text{Te}_3)_{1-y}(\text{In}_2\text{Te}_3)_y$ (up to $y = 25$ mol.%) [1, 8]. According to our assumption, introduction of this compound into a ternary solid solution $(\text{Bi}_2\text{Te}_{3-x}\text{Se}_x)_{1-y}(\text{In}_2\text{Te}_3)_y$ -In ($x = 0.15$ and 0.3) doped with halogenides was also to bring about a decrease in crystal lattice thermal conductivity κ_L of material and an increase in E_g , T_{\max} and Z_{\max} (scheme I, at $E_F - \text{const}$) (Fig. 1). The results of the work

demonstrated that an assumption of the possibility of expanding the working interval towards higher temperatures is met in $(Bi_2Te_{3-x}Se_x)_{1-y}(In_2Te_3)_y < SbI_3 >$ alloys only partially, in the range of low indium concentrations (up to $y \leq 0.1 - 0.2$ mol.% In_2Te_3). For these alloys, the thermoelectric figure of merit Z increased from $0.0029 - 0.003$ to $0.0031 - 0.0032$ 1/K and Z_{\max} position shifted by $\Delta T = 10 - 30$ K towards higher temperatures. With increasing indium content in solid solution $y > 0.2$ mol.% In_2Te_3 , Z_{\max} of alloys drastically decreased to 0.002 1/K, and Z_{\max} position shifted towards lower temperatures.

1. Experiment

The Czochralski technique was used to grow single crystals of $(Bi_2Te_{3-x}Se_x)_{1-y}(In_2Te_3)_y < SbI_3 >$ ($x = 0.15$ and 0.3) solid solution doped with $< SbI_3 >$ and In_2Te_3 ($y = 0.1; 0.2; 0.5; 1.0; 2.0$ mol.%) (Table 1). The SbI_3 and In_2Te_3 compounds had been pre-synthesized in evacuated quartz ampoules. Indium was introduced into charge material in amounts from $y = 0.1$ to 2 mol. % In_2Te_3 . The $< SbI_3 >$ dopant was introduced in the amount ($a_I = 0 - 0.17$ at.% I), so as to assure the optimal current carrier concentration for temperatures $T = 300$ K ($x = 0.15$, $n \sim 1.5 \cdot 10^{19}$ cm $^{-3}$) and $T = 300 - 400$ K ($x = 0.3$, $n \sim 2 \cdot 10^{19}$ cm $^{-3}$) [1, 7]. Indium creates donor levels in bismuth and antimony chalcogenides [1], so with increasing its content in solid solution, the amount of halogenide was reduced with a view to retain the optimal thermoEMF $\alpha_{300\text{K}} \sim 210$ $\mu\text{V/K}$ for alloys with $x = 0.15$ and $\alpha_{300\text{K}} \sim 190$ $\mu\text{V/K}$ for alloys with $x = 0.3$.

The thermoelectric characteristics were measured by compensation method on rectangular samples of dimensions $8 \times 8 \times 16$ mm 3 cut out in direction perpendicular to trigonal crystal axis. The Seebeck coefficient α , electrical conductivity σ and thermal conductivity κ of samples were measured in the temperature range of $T = 100 - 400$ K. The measuring sensitivity was $\Delta T \sim 0.01$ K; $\Delta\alpha \sim 2$ $\mu\text{V/K}$, $\Delta\sigma \sim 10$ S/cm, $\Delta\kappa \sim 0.003$ W/(cm·K), the accuracy of measuring the absolute values of said characteristics was at least $\Delta T \sim 0.5$ K; $\delta\alpha, \delta\sigma \sim 3\%$; $\delta\kappa \sim 5\%$. Based on the results of measuring α , σ and κ , the value of thermoelectric figure of merit Z of materials was calculated by formula (1). The sensitivity of measuring Z value by means of employed procedure was $\sim 5\%$ (± 0.00007 1/K), the accuracy of absolute Z values obtained was about $\sim 14\%$ (± 0.0002 1/K).

The energy gap width E_g of solid solutions was estimated according to Vegard's law based on the tabulated data for binary compounds [8], the Fermi energy E_F of samples was determined by thermoEMF method according to $\alpha_{300\text{K}}$ value measured experimentally (Table 1) [1].

2. Experimental results and their discussion

2.1 Band parameters of alloys

The band parameters of n - $(Bi_2Te_{3-x}Se_x)_{1-y}(In_2Te_3)_y < SbI_3 >$ ($x = 0.15$ and 0.3) alloys prior to and after their doping with indium are given in Table 1. The general pattern of change in the band structure of alloys on doping is shown in Fig. 2. From Table 1 it is seen that all the investigated alloys had thermoEMF $\alpha_{300\text{K}} \sim 210$ $\mu\text{V/K}$ for $x = 0.15$ and $\alpha_{300\text{K}} \sim 190$ $\mu\text{V/K}$ for $x = 0.3$, optimal for temperatures $T = 300$ and $300 - 400$ K, respectively [1]. The Fermi energies of resulting alloys had approximately identical values within each series of compositions – $E_F \sim 0.01$ eV for $x = 0.15$ and $E_F \sim 0.001$ eV for $x = 0.3$. The E_F values of all the alloys were in the energy gap close to conduction-band edge and did not change with increase in doping degree (Fig. 2) [1]. On the other hand, with increase in doping degree $y = 0 \rightarrow 2$ mol.% In_2Te_3 , the energy gap width E_g of alloys with $x = 0.15$ and 0.3 increased by $11 - 12\%$ ($a \rightarrow b$, Fig. 2). Thus, condition $E_F - \text{const}$ necessary for studying the effect produced by onset of transition to intrinsic conduction on the thermoelectric figure of merit Z of alloys on doping ($1 \rightarrow 2 \rightarrow 3$, Fig. 1) was fulfilled in the work with sufficient precision.

Table 1

Compositions and band parameters of investigated n - $(Bi_2Te_{3-x}Se_x)_{1-y}(In_2Te_3)_y < SbI_3 >$ alloys

№	Composition, y , mol.%	ThermoEMF, $\alpha_{300\text{ K}}$, $\mu\text{V/K}$		Energy gap width, E_g , eV		Fermi energy, E_F , eV [*])	
		$x = 0.15$	$x = 0.3$	$x = 0.15$	$x = 0.3$	$x = 0.15$	$x = 0.3$
1	0	214	190	0.161	0.162	-0.011	-0.003
2	0.1	214	185	0.162	0.163	-0.011	-0.002
3	0.2	210	178	0.163	0.164	-0.010	-0.001
4	0.5	214	190	0.166	0.167	-0.011	-0.003
5	1.0	193	180	0.170	0.172	-0.004	-0.001
6	2.0	192	180	0.179	0.182	-0.004	-0.001

^{*}) Counting of E_F , energy from the edge of conduction band

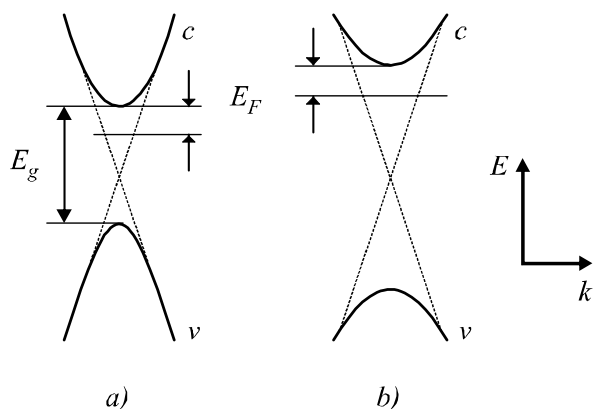


Fig. 2. Pattern of change in the band structure of investigated n - $(Bi_2Te_{3-x}Se_x)_{1-y}(In_2Te_3)_y < SbI_3 >$ alloys doped with indium (a \rightarrow b). Bands: c is conduction band, v is valence band, E_g is energy gap. E_F is the Fermi energy.

2.2. Thermoelectric characteristics of alloys

Based on the separate measurements of α , σ and κ , from formula (1) there were calculated temperature dependences of thermoelectric figure of merit Z for $(Bi_2Te_{3-x}Se_x)_{1-y}(In_2Te_3)_y < SbI_3 >$ ($x = 0.15$ and 0.3) crystals. Fig. 3 shows $Z = f(T)$ dependences of $(Bi_2Te_{3-x}Se_x)_{1-y}(In_2Te_3)_y < SbI_3 >$ samples with $x = 0.15$ (a) and $x = 0.3$ (b) without In_2Te_3 and with the content $y = 0.1$; 0.2 and 0.5 mol.% In_2Te_3 in the charge material. According to Fig. 3, $Bi_2Te_{2.85}Se_{0.15}$ (a) and $Bi_2Te_{2.7}Se_{0.3}$ (b) samples comprising 0.1 and 0.2 mol.% In_2Te_3 in the charge material (0.04 and 0.08 at.% of indium, respectively), possess higher thermoelectric figure of merit Z in the temperature range of $T = 300 - 400$ K than prototype alloys undoped with indium (curves 2). Maximum Z_{\max} values 0.0032 and 0.0031 K $^{-1}$ were observed for alloys with small indium dopants $(Bi_2Te_{2.85}Se_{0.15})_{0.999}(In_2Te_3)_{0.001} < SbI_3 >$ and $(Bi_2Te_{2.7}Se_{0.3})_{0.998}(In_2Te_3)_{0.002} < SbI_3 >$, respectively. The afore-referenced Z_{\max} values were attained at temperature $T_{\max} \sim 300$ and 330 K shifted by 10 and 30 K towards higher temperatures as compared to prototype alloys ($y = 0$) (curves 1, Fig. 3). The results of comparing the thermoelectric properties of the best indium-doped sample $(Bi_2Te_{2.7}Se_{0.3})_{0.998}(In_2Te_3)_{0.002} < SbI_3 >$ ($y = 0.2$) and the initial prototype alloy in the temperature range of $T = 220 - 373$ K are represented in Table 2.

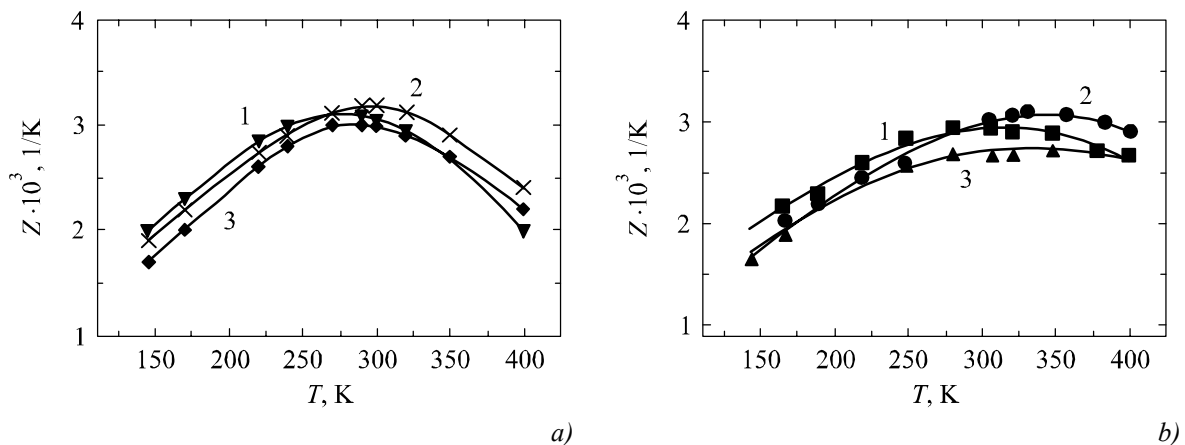


Fig. 3. Temperature dependences of thermoelectric figure of merit Z of $(\text{Bi}_2\text{Te}_{3-x}\text{Se}_x)_{1-y}(\text{In}_2\text{Te}_3)_y <\text{SbI}_3>$ alloys. x : a – 0.15; b – 0.3; y : 1 – 0; 2 (a) – 0.001; 2 (b) – 0.002; 3 – 0.005.

Table 2

Thermoelectric properties of single crystals in the temperature range of 220 – 370 K

No	Solid solution composition	T , K	α , $\mu\text{V}/\text{K}$	σ , S/cm	$\kappa \cdot 10^3$, $\text{W}/(\text{cm} \cdot \text{K})$	$Z \cdot 10^3$, $1/\text{K}$
1	$\text{Bi}_2\text{Te}_{2.7}\text{Se}_{0.3} <\text{SbI}_3>$	223	– 156	1760	18.2	2.4
		273	– 183	1380	16.6	2.8
		323	– 204	1050	15.2	2.9
		373	– 219	910	15.4	2.8
2	$(\text{Bi}_2\text{Te}_{2.7}\text{Se}_{0.3})_{0.998}$	223	– 156	2211	20.9	2.5
	$(\text{In}_2\text{Te}_3)_{0.002} <\text{SbI}_3>$	273	– 179	1700	20.0	2.7
		323	– 203	1330	17.6	3.1
		373	– 207	1270	18.3	3.0

However, growth of Z_{\max} was observed only with a low level of alloy doping $y \leq 0.1 - 0.2$ mol.% In_2Te_3 (Fig. 3). With increasing indium content in solid solution $y > 0.1 - 0.2$ mol.% In_2Te_3 , Z_{\max} values of alloys drastically decreased (curves 3, Fig. 3). On the concentration dependences of thermoelectric properties of samples with the growth of $y = 0.2 \rightarrow 2$ mol.% In_2Te_3 there was a decrease in $Z = (3.1 - 3.2) \rightarrow 2.0 \text{ K}^{-1}$ (curves 9, 10, Fig. 4), and T_{\max} value ($310 - 330 \rightarrow 275$ K in this case shifted towards low temperatures (curves 3, 4, Fig. 5).

2.3. Concentration dependences of thermoelectric properties

Fig. 4 shows the concentration dependences of electrical conductivity σ (1, 2), thermoEMF α (3, 4), thermal conductivity κ (5, 6) and estimated values of lattice thermal conductivity κ_L (7, 8) and thermoelectric figure of merit Z (9, 10) on the composition of investigated alloys $(\text{Bi}_2\text{Te}_{3-x}\text{Se}_x)_{1-y}(\text{In}_2\text{Te}_3)_y <\text{SbI}_3>$ ($x = 0.15$ and 0.3) (Table 1) at room temperature.

The κ_L value (7, 8, Fig. 4) was calculated by means of the Wiedemann-Franz law $\kappa_e = L\sigma T$ (here L is the Lorentz number, σ is electrical conductivity) allowing for the onset of transition of alloys to intrinsic conduction ($\kappa = \kappa_L + \kappa_e + \kappa_b$, here κ_L , κ_e and κ_b are the lattice, electron and bipolar thermal conductivities, respectively). The Lorentz number L was calculated in the approximation of parabolic bands and the elastic mechanism of current carrier scattering, the κ_b value was estimated according to the formula of Davydov and Shmushkevich [1].

Fig. 5 shows dependences of maximum thermoelectric figure of merit temperature T_{\max} (1 – 4), electron mobility μ_e at room temperature (5 – 6), the ratio of electron and hole partial conductivities $B = \sigma_n/\sigma_p$ (7, 8) and parameter A (9, 10) appearing in expression (3) on indium content in the samples. T_{\max} value (3, 4, Fig. 5) was determined experimentally from the temperature dependences $Z = f(T)$, then, with regard to E_g and E_F values of alloys (Table 1), parameter A was calculated (9, 10) from formula (3). The value of electron mobility (curves 5, 6, Fig. 5) was estimated from formula $\mu_n = \sigma/(en)$ with regard to experimental σ values (curves 1, 2, Fig. 4) for electron concentration $n \sim 1.5$ and $2.10^{19} \text{ cm}^{-3}$ assumed to be equal for samples $x = 0.15$ and 0.3 with different $y = 0 – 2 \text{ mol.}\%$ In_2Te_3 . The ratio of partial electron and hole conductivities $B = \sigma_n/\sigma_p$ (7, 8, Fig. 5) was determined using thermoEMF method by the deviations of $\alpha = f(T)$ dependences from theoretical ones corresponding to impurity conduction region of samples. The α values in the region of intrinsic conduction were calculated from the formula of two-band model $\alpha = (\alpha_n + B\alpha_p)/(1 + B)$ (here α_n and α_p are partial thermoEMF of electrons and holes) [1]. The parabolic band approximation and band parameters of alloys listed in Table 1 were used in the calculations.

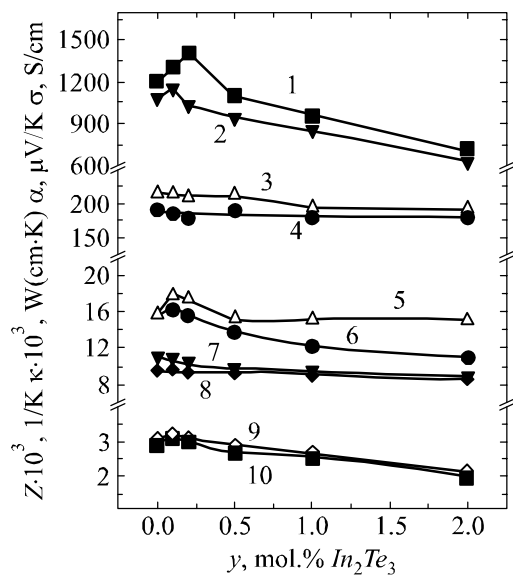


Fig. 4. Dependences of electrical conductivity σ (1, 2), thermoEMF α (3, 4), thermal conductivity κ (5, 6), its lattice component κ_l (7, 8) and thermoelectric figure of merit Z_{\max} (9, 10) on indium content in $(\text{Bi}_2\text{Te}_{3-x}\text{Se}_x)_{1-y}(\text{In}_2\text{Te}_3)_y$ alloys of different composition. $x, \text{ mol.}\% \text{ Bi}_2\text{Se}_3: 2, 3, 6, 7, 9 - 0.15; 1, 4, 5, 8, 10 - 0.3$ ($T = 300 \text{ K}$).

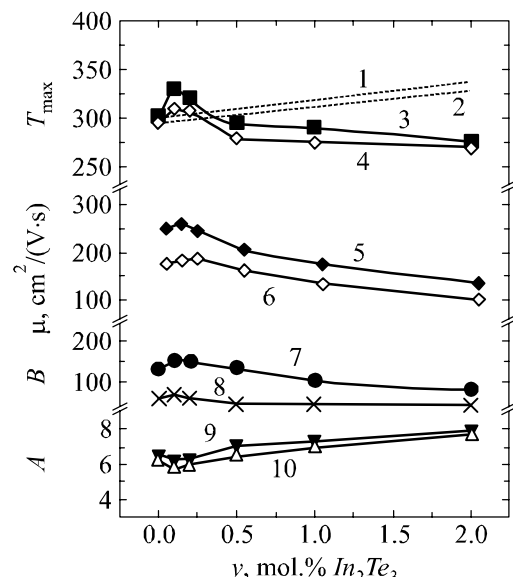


Fig. 5. Dependences of maximum thermoelectric figure of merit temperature T_{\max} (1 – 4), electron mobility μ_e (5 – 6), conductivity ratio $B = \sigma_n/\sigma_p$ ($T = 300 \text{ K}$) (7, 8) and parameter A (formula (3)) (9, 10) on indium content y in $(\text{Bi}_2\text{Te}_{3-x}\text{Se}_x)_{1-y}(\text{In}_2\text{Te}_3)_y$ alloys, $x, \text{ mol.}\% \text{ Bi}_2\text{Se}_3: 2, 4, 5, 8, 9 - 0.15; 1, 3, 6, 7, 10 - 0.3$. 1, 2 – calculation according to formula (3) at A ($y = 0$) ~ 6.3 and 6.5 .

From Fig. 4 – 5 it is seen that the concentration dependences of thermoelectric properties of investigated $(\text{Bi}_2\text{Te}_{3-x}\text{Se}_x)_{1-y}(\text{In}_2\text{Te}_3)_y$ -SbI₃ alloys ($x = 0.15$ and 0.3) on indium content at room temperature

have specific features at $y = 0.1 - 0.2$ mol.% In_2Te_3 . On the curves σ , κ , $Z = f(y)$ on the background of general reduction of properties with the growth of y due to a decrease in electron mobility μ_e on doping of In_2Te_3 alloys [1, 6], local maxima were also observed at $y = 0.1 - 0.2$ mol.% In_2Te_3 (curves 1, 2, 5, 6, 9, 10, Fig. 4). On the concentration dependence of parameter A at the same compositions there was a local minimum (9, 10, Fig. 5). Comparison of the experimental and estimated dependences $T_{\max} = f(y)$ (curves 1 and 2, 3 and 4, Fig. 5) shows that local growth of T_{\max} and A minimum at $y = 0.1 - 0.2$ mol.% In_2Te_3 is not directly related to increase in E_g of solid solutions (Table 1).

We attribute the curve features (Fig. 4 – 5) to local growth of electron mobility μ_e at $y = 0.1 - 0.2$ mol.% In_2Te_3 (curve 5, 6, Fig. 5) increasing parameter $B = \sigma_n/\sigma_p$ (curves 7 and 8, Fig. 6). The growth of B , in turn, decreases the value of parameter A and shifts T_{\max} towards high temperatures (curves 9, 10 and 3, 4, Fig. 6). On curves κ_L the corresponding anomaly was less pronounced, which indicates a weaker change in phonon scattering in crystals on introduction of $y = 0.1 - 0.2$ mol.% In_2Te_3 (curves 7, 8, Fig. 4). As a result, at $y = 0.1 - 0.2$ mol.% In_2Te_3 the ratio μ_n/κ_L was increased, hence leading to a local increase in Z_{\max} of samples (curves 9, 10, Fig. 4). The results obtained (Fig. 3 – 5) can be explained on the basis of known mechanisms of dopants introduction into solid solutions based on bismuth and antimony chalcogenides [1, 7].

2.3. Solid solution doping mechanisms

The initial crystalline structure for $(\text{Bi}_2\text{Te}_{3-x}\text{Se}_x)_{1-y}(\text{In}_2\text{Te}_3)_y <\text{SbI}_3>$ solid solutions ($x = 0.15$ and 0.3) is Bi_2Te_3 crystalline structure (space group of $R\bar{3}m$ symmetry) which is a set of complex layers – $(-\text{Te}^{(1)} - \text{Bi} - \text{Te}^{(2)} - \text{Bi} - \text{Te}^{(1)})-$ quintets alternating in direction perpendicular to crystal trigonal axis [1]. Characteristics of ions entering $(\text{Bi}_2\text{Te}_{3-x}\text{Se}_x)_{1-y}(\text{In}_2\text{Te}_3)_y <\text{SbI}_3>$ solid solution, their most probable positions in crystal lattice and the respective electric activity in solid solution are given in Table 3 [1, 7 – 9]. In the lattice of $((\text{Bi}_2\text{Te}_{3-x}\text{Se}_x)_{1-y}(\text{In}_2\text{Te}_3)_y <\text{SbI}_3>$ solid solution indium occupies the places of bismuth or is in the interstitial sites where it exhibits a donor effect (Table 3) [1].

Table 3

*Characteristics of ions entering
 $(\text{Bi}_2\text{Te}_{2.7}\text{Se}_{0.3})_{1-x}(\text{In}_2\text{Te}_3)_x <\text{SbI}_3>$ solid solution [1, 7 – 9]*

Ion	Bi^{+3}	Sb^{+3}	In^{+3}	Te^{-2}	Se^{-2}	Γ^1
Ionic radius $r, \text{\AA}$	1.20	0.90	0.92	2.11	1.93	2.20
Atomic mass m, g	208.98	121.75	114.82	127.60	77.96	126.90
Positions in the lattice and electrical activity	$[\text{Bi}]_{\text{Bi}}(0)$ $[\text{Bi}]_{\text{Te}}(3e/5)$	$[\text{Sb}]_{\text{Bi}}(0)$	$[\text{In}]_{\text{Bi}}(0)$ $[\text{In}]_{\text{Bi}}(1e)$	$[\text{Te}]_{\text{Te}}(0)$	$[\text{Se}]_{\text{Te}}(0)$	$[\text{I}]_{\text{Te}}(1e)$

These violations in cation sublattice reduce current carrier mobility μ_e and decrease lattice thermal conductivity κ_L due to additional scattering of electrons and phonons on the impurities and cation vacancies which grow in number with increasing In_2Te_3 content [1, 7, 10]. As a result, at

$y > 0.2$ mol.% In_2Te_3 , σ , κ_L and μ_n values decrease with the growth of y which leads to a total reduction of Z (Fig. 5 – 6). On the other hand, local growth of Z at $y \sim 0.1 - 0.2$ mol.% In_2Te_3 (curves 9, 10, Fig. 5) is related to peculiarities on σ , κ_L and μ_n curves (Fig. 4 – 5) at low y which can be explained by a change in the concentration ratio of dopants (In , I and Sb) in the samples, as long as in synthesis of alloys, on addition of In_2Te_3 , we simultaneously reduced the concentration of $\langle \text{SbI}_3 \rangle$ in charge material. The $\langle \text{SbI}_3 \rangle$ dopant dissociates in solid solution, in which case Sb^{+3} ions occupy predominantly the places of Bi^{+3} , and I^- ions – predominantly the places of $\text{Te}^{(2)}$ where they are donors (Table 3) [1]. I^- ions scatter electrons and phonons in bismuth and antimony chalcogenides more intensively than In^{+3} and Sb^{+3} which is related to different dimensions, masses and charge state of ions (Table 3) [1]. Therefore, in the region of $y > 0$, with the growth of indium amount and a reduction of iodine amount, the electron mobility in samples μ_n can be increased. Possible growth mechanism of the electron mobility μ_n with a complex doping of samples is represented in Fig. 6.

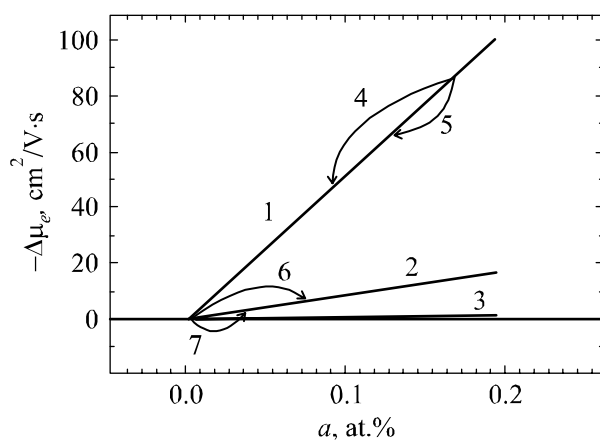


Fig. 6. Change in electron mobility $\Delta\mu_e$ (1 – 3) of $(\text{Bi}_2\text{Te}_{2.7}\text{Se}_{0.3})_{1-x}(\text{In}_2\text{Te}_3)_x$ - $\langle \text{SbI}_3 \rangle$ alloys on introduction of dopant a : 1, 4, 5 – I ; 2, 6, 7 – In ; 3 – Sb [11]. 5 and 7; 4 and 6 – complex doping of In samples with a simultaneous reduction of the amount of introduced I . 5 and 7 – $x = 0.15$, $y = 0.1$ mol.% In_2Te_3 ; 4 and 6 – $x = 0.3$, $y = 0.2$ mol.% In_2Te_3 .

According to [1], with a separate introduction into bismuth and antimony chalcogenides of small In , I and Sb dopants, the electron mobility reduction is $d\mu_e/da = -83$; -500 and -8 $\text{cm}^2/(\text{V}\cdot\text{s})$ per $a = 1$ at.% of introduced impurity (dependences 1 – 3, Fig. 6). Assuming that each In^{3+} and I^- ion introduced into solid solution gives 1 electron into conduction band [1], we obtain that at $y = 0 \rightarrow 0.2$ mol.% In_2Te_3 ($\Delta a_{\text{In}} = 0.08$ at.% In) the iodine and antimony concentration in charge material was reduced by $\Delta a_I = -0.8$ at.% I and $\Delta a_{\text{Sb}} \sim -0.026$ at.% Sb , respectively. Hence, in the approximation of independent electron scattering by different impurities we get estimates of the value of local growth of electron mobility $\Delta\mu_n \sim 15$ and 30 $\text{cm}^2/(\text{V}\cdot\text{s})$ for alloys with $y = 0.1$ and 0.2 mol.% In_2Te_3 , which is in agreement with the experiment (curves 5, 6, Fig. 5). In so doing, all specific features of thermoelectric characteristics of alloys at $y = 0.1$ and 0.2 mol.% In_2Te_3 (Fig. 4 – 5) can be explained by the substitution of one donor dopant (I) with the other (In), less reducing electron mobility μ_n in solid solution (Fig. 7). Thus, the observed local growth of Z_{\max} and T_{\max} at $y = 0.1$ and 0.2 mol.% In_2Te_3 is due to a shift of the onset of intrinsic conduction of samples towards high temperatures, caused by local growth of μ_n and B and a reduction of parameter A on introduction of indium and a simultaneous reduction of halogenide concentration in solid solution (curves 5 – 10, Fig. 5) [11].

2.4. Extrinsic and intrinsic conduction regions

Fig. 7 shows the temperature dependences of dimensionless figure of merit ZT in extrinsic ($T < 300 - 400$ K) and intrinsic ($T > 300 - 400$ K) conduction regions of the best of indium-doped alloys ($\text{Bi}_2\text{Te}_{2.85}\text{Se}_{0.15})_{0.999}(\text{In}_2\text{Te}_3)_{0.001}$ $<\text{SbI}_3>$ and ($\text{Bi}_2\text{Te}_{2.7}\text{Se}_{0.3})_{0.998}(\text{In}_2\text{Te}_3)_{0.002}$ $<\text{SbI}_3>$ (curves 3 and 1) as compared to prototype alloys ($y = 0$) ($x = 0.15$ and 0.3) (curves 4 and 2). Extrapolation of curves 3 and 1 (Fig. 7) towards high temperatures (dotted line) was done by the Gauss method. From Fig. 7 it is seen that for ($\text{Bi}_2\text{Te}_{2.7}\text{Se}_{0.3})_{0.998}(\text{In}_2\text{Te}_3)_{0.002}$ $<\text{SbI}_3>$ alloy ZT value reaches 1.2 at $T = 400$ K (curve 1)¹. It is $\sim 20\%$ higher than $ZT \sim 0.9$ of prototype alloy (curve 2, Fig. 7) and $\sim 10\%$ higher than ZT values $\sim 1.10 - 1.12$ estimated for the best bulk nanostructured polycrystalline samples $p\text{-Bi}_x\text{Sb}_{2-x}\text{Te}_3$ with their thermal conductivity $\kappa \sim 0.009$ W/(cm·K) approaching the thermal conductivity of “phonon glass” ($\kappa \sim 0.005$ W/(cm·K)) [12].

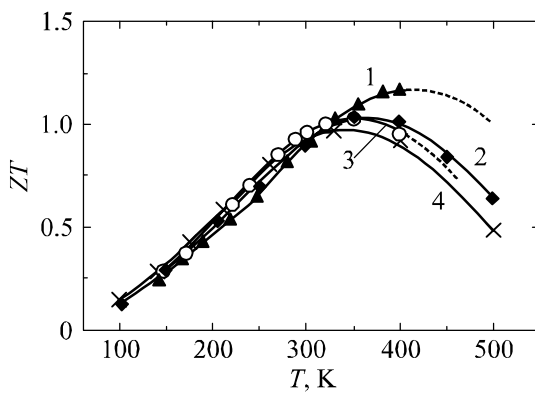


Fig. 7. Temperature dependences of dimensionless figure of merit ZT of $(\text{Bi}_2\text{Te}_{3-x}\text{Se}_x)_{1-y}(\text{In}_2\text{Te}_3)_y$ alloys. x , mol.% Bi_2Se_3 : 3, 4 – 0.15; 1, 2 – 0.3. y , mol.% In_2Te_3 : 2, 4 – 0; 3 – 0.1; 1 – 0.2.

Moreover, further increase in Z and ZT of resulting alloys is possible due to the Thomson effect [4]. In operation at considerable temperature differences ΔT , the bulk Thomson thermoEMF gradients $\nabla\alpha_\tau$ act in thermoelement legs, changing Z of devices [4, 13, 14]. The scheme of origination of the Thomson effect $\nabla\alpha_\tau$ in TEG and TEH in the regions of extrinsic (a) and intrinsic (b) conduction of legs is shown in Fig. 8. From Fig. 8 it follows that in TEG and TEH the Thomson effect increases Z in the region of intrinsic conduction of legs (b) ($\nabla\alpha_{tn} \uparrow \nabla\alpha_{tp} \uparrow \nabla\alpha$) and decreases Z in the region of extrinsic conduction of legs (a) ($\nabla\alpha_{tn} \uparrow \nabla\alpha_{tp} \downarrow \nabla\alpha$). The action of the Thomson effect is related to increase and decrease of contact thermoEMF $\nabla\alpha$ on the side of the bulk ($\nabla\alpha_{tn}$ and $\nabla\alpha_{tp}$), respectively. In TEC, the action of the Thomson effect on Z of devices is changed to the opposite [4].

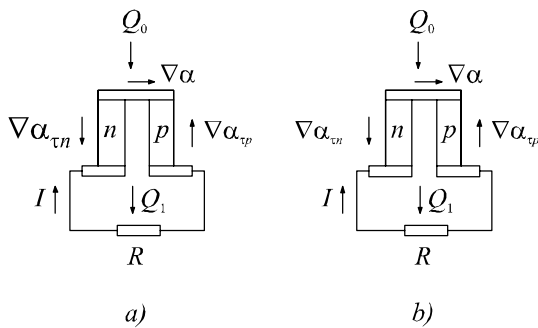


Fig. 8. The scheme of origination of the Thomson effect $\nabla\alpha_\tau$ in TEG and TEH in extrinsic (a) and intrinsic (b) conduction regions of legs. a – $\nabla\alpha_{tn} \uparrow \nabla\alpha_{tp} \downarrow \nabla\alpha$; b – $\nabla\alpha_{tn} \uparrow \nabla\alpha_{tp} \uparrow \nabla\alpha$. R – load resistance [4].

¹ From condition $Z \approx Z_{\max}$ at $T = T_{\max} \pm 50$ K follows the ratio $T_{\max}(ZT) \approx T_{\max} + 100$ K.

Fig. 9 shows the temperature dependences of thermoEMF α (1 – 4) and thermoEMF difference $\Delta\alpha$ arising at temperature difference on the sample $\Delta T = 100$ K (5, 6), for $(Bi_2Te_{2.85}Se_{0.15})_{0.999}(In_2Te_3)_{0.001}$ $< SbI_3 >$ and $(Bi_2Te_{2.7}Se_{0.3})_{0.998}(In_2Te_3)_{0.002}$ $< SbI_3 >$ alloys, as well as prototype samples ($y = 0$). Fig. 10 shows corrections to figure of merit Z^*/Z of TPC with the legs of $Bi_2Te_{3-x}Se_x$ type alloys occurring due to the Thomson effect. The value of corrections was calculated by the formula $Z^*/Z \approx (1 + \Delta\alpha / 2\alpha)$ (here $\Delta\alpha = \Delta\alpha_n = \Delta\alpha_p$ and α are thermoEMF differences on the legs and thermocouple junction) [13]. From Fig. 10 it can be seen that in operation of $(Bi_2Te_{2.85}Se_{0.15})_{0.999}(In_2Te_3)_{0.001}$ $< SbI_3 >$ and $(Bi_2Te_{2.7}Se_{0.3})_{0.998}(In_2Te_3)_{0.002}$ $< SbI_3 >$ alloys as the legs of TEG and TEH, Z value of devices will further increase by $\sim 5 - 10\%$ at temperature $T = 550$ K due to the Thomson effect ($\Delta T = 100$ K). With increase in ΔT within the intrinsic conduction region ($T > 300 - 400$ K), Z^*/Z value will grow further [4, 13, 14].

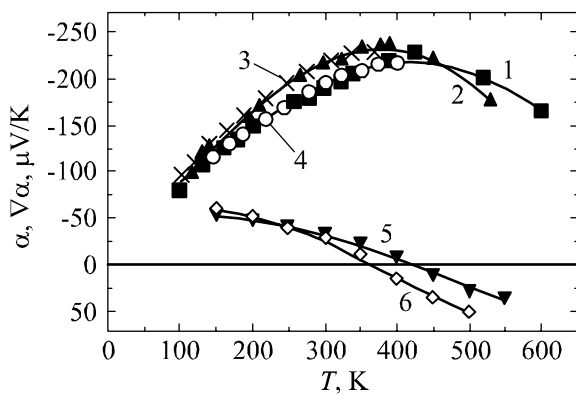


Fig. 9. Temperature dependences of thermoEMF α (1 – 4) and thermoEMF difference $\Delta\alpha$ at temperature difference on the sample $\Delta T = 100$ K (5, 6) for $(Bi_2Te_{3-x}Se_x)_{1-y}(In_2Te_3)_y$ alloys of different composition x , mol.% Bi_2Se_3 : 2, 4, 6 – 0.15; 1, 3, 5 – 0.3. y , mol.% In_2Te_3 : 1, 2, 5, 6 – 0; 4 – 0.1; 3 – 0.2.

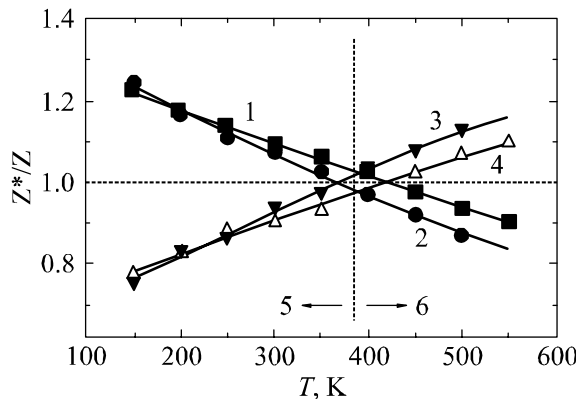


Fig. 10. Corrections to figure of merit Z^*/Z of thermoelectric power converters (TPC) with the legs of $Bi_2Te_{3-x}Se_x$ type alloys due to the Thomson effect ($\Delta T = 100$ K). x , mol.% Bi_2Se_3 : 2, 3, – 0.15; 1, 4 – 0.3. Conduction of legs: 5 – extrinsic; 6 – intrinsic. 1, 2 – TEC; 3, 4 – TEG.

3. Conclusion

In the present work, the Czochralski technique with liquid phase replenishment was used to prepare single crystals of n - $(Bi_2Te_{3-x}Se_x)_{1-y}(In_2Te_3)_y$ ($x = 0.15$ and 0.3) solid solutions doped with In_2Te_3 compound ($y = 0 - 2$ mol.%). Processes of complex doping solid solutions with small

In_2Te_3 and $\langle \text{SbI}_3 \rangle$ dopants possessing a donor effect have been studied. The dopants were introduced into a solid solution in the amount assuring the optimal electron concentration for temperatures $T = 300$ and $300 - 400$ K. To maintain the optimal electron concentration in the samples with increase in In_2Te_3 content, the amount of $\langle \text{SbI}_3 \rangle$ in charge material was decreased. It was established that with the growth of $y > 0.2$ mol.% In_2Te_3 , the electrical conductivity σ and lattice thermal conductivity κ_L decrease due to a change in the band structure and the growth of impurity scattering of electrons and phonons in the samples [1]. At $y \sim 0.1 - 0.2$ mol.% In_2Te_3 , the curves of thermoelectric characteristics of samples versus indium content had specific features attributed in this work to a change in the concentration ratio of $\langle \text{SbI}_3 \rangle$ and In_2Te_3 dopants in solid solution. In the region $y \leq 0.1 - 0.2$ mol.% In_2Te_3 there was local growth of electron mobility μ_e and a slight decrease of κ_L . As a result, for alloys with $x = 0.15$ and 0.3 and $y = 0.1 - 0.2$ mol.% In_2Te_3 the value of thermoelectric figure of merit Z increased from $0.0029 - 0.003$ to $0.0031 - 0.0032$ 1/K, and Z_{\max} position shifted by $\Delta T = 10 - 30$ K towards high temperatures. Because of joint action of two said factors the dimensionless figure of merit of the best of investigated alloys $(\text{Bi}_2\text{Te}_{2.7}\text{Se}_{0.3})_{0.998}(\text{In}_2\text{Te}_3)_{0.002} \langle \text{SbI}_3 \rangle$ increased by $\sim 30\%$ and reached $(ZT)_{\max}$ values $0.87 \rightarrow 1.2$ at $T = 400$ K that were of practical interest.

Thus, in this work we show the possibility of increase in Z_{\max} and $(ZT)_{\max}$ of bismuth and antimony chalcogenide alloys with the onset of intrinsic conduction of samples shifted towards high temperatures (arrow I, Fig. 1) [11]. However, the growth of Z_{\max} and $(ZT)_{\max}$ observed in operation under condition of $E_F - \text{const}$ (Fig. 3 and 7) was not directly related to the growth of the energy gap width of solid solution E_g , but was determined by local growth of electron mobility μ_e (curves 5, 6, Fig. 5). With further increase in y from 0.2 to 2 mol.% In_2Te_3 , despite the growth of E_g (Table 1), Z_{\max} value of alloys drastically decreased to 0.002 1/K because of reduced electron mobility μ_e , and Z_{\max} position shifted towards low temperatures (curves 3, 4, Fig. 5).

On doping narrow-gap materials based on bismuth and antimony chalcogenides ($E_g = 0.1 - 0.2$ eV), reduction of electron mobility $\mu_e = e\langle\tau\rangle/m_c$ can be defined by two main factors: 1) decrease in the average electron relaxation time $\langle\tau\rangle$ with increase in impurity scattering; 2) increase in effective electron conduction mass $m_c = d^2E/dk^2$ with increase in E_g ($a \rightarrow b$, Fig. 2) [1]. The specific feature of bismuth and antimony chalcogenides is different position of electron and hole extremes in quasi-impulse space [1], so that with increase in E_g in the region of $y > 0.2$ mol.% In_2Te_3 , the contribution of electron current carriers to electrical conductivity of crystals decreased to a larger extent than that of holes (7, 8, Fig. 5). As a result of joint action of all above-mentioned factors, the onset of samples transition to intrinsic conduction shifted towards low temperatures, so in implementing the intended scheme of doping bismuth and antimony chalcogenides (arrow I, Fig. 1) using indium as a dopant we have succeeded only partway.

Acknowledgement. We express gratitude to P.P. Konstantinov (A.F. Ioffe Physics and Technical Institute) for the measurements of temperature dependences of thermoelectric properties of alloys.

References

1. B.M. Goltsman, V.A. Kudinov and V.A. Smirnov, Semiconductor Thermoelectric Materials Based on Bi_2Te_3 (Nauka, Moscow, 1972).
2. C.B. Vining, Restricted Opportunities of Thermoelectricity Under Climatic Crisis Conditions, J. Thermoelectricity 4, 7 – 20 (2008).
3. L.I. Anatychuk, V.A. Semenyuk, Optimal Control Over Properties of Thermoelectric Materials and Devices (Prut, Chernivtsi, 1992).
4. M.A. Korzhuev, Symmetry Analysis of Thermoelectric Energy Converters with Inhomogeneous

- Legs, J. Electronic Materials 39 (9), 1381 – 1385 (2010).
5. T.E. Svechnikova, N.M. Maksimova, P.P. Konstantinov, Doping with Bismuth Sulfide of Single Crystals of Solid Solutions Based on Bi_2Te_3 , Neorganicheskiye Materialy 34 (3), 302 – 305 (1998).
 6. T.E. Svechnikova, P.P. Konstantinov, G.T. Alekseeva, Electrophysical Properties of $\text{Bi}_2\text{Te}_{2.85}\text{Se}_{0.15}$ Solid Solutions Doped with Cu , Cd , In , Ge , Sn , Se , Neorganicheskiye Materialy 36 (6), 677 – 681 (2000).
 7. V.A. Kutasov, L.N. Lukyanova, M.V. Vedernikov, Shifting the Maximum Figure of Merit of $(\text{Bi}, \text{Sb})_2(\text{Te}, \text{Se})_3$ Thermoelectrics to Lower Temperatures. In: Thermoelectric Handbook. Macro to Nano. Ed. D.M. Rowe (Tailor & Francis, London-N.Y., 2006).
 8. Physicochemical Properties of Semiconductor Substances. Handbook. Ed. A.V. Novoselova (Nauka, Moscow, 1979).
 9. G.B. Bokiy, Introduction to Chrystal Chemistry (MSU, Moscow, 1954).
 10. H. Scherrer, S. Scherrer, Thermoelectric Properties of Bismuth Antimony Telluride Solid Solutions. In: Thermoelectric Handbook. Macro to Nano. Ed. D.M. Rowe London (Taylor & Francis, London-N.Y., 2006).
 11. M.A. Korzhuev, Concomitant Effects in High-Performance Thermoelectric Materials, Vysokochistye Veschestva 2, 74 – 89 (1996).
 12. L.P. Bulat, D.A. Pshenai-Severin, I.A. Drabkin, V.V. Karataev, V.B. Osvensky, Yu.N. Parkhomenko, V.D. Blank, G.I. Pivovarov, V.T. Bublik, and N.Yu. Tabachkova, Mechanisms of Thermoelectric Figure of Merit Increase in the Bulk Nanostructured Polycrystals, J. Thermoelectricity 1, 14 – 19 (2011).
 13. M.A. Korzhuev, L.D. Ivanova, Yu.V. Granatkina, On the Operational Efficiency of Inhomogeneous Thermoelement in the Mode of Joule Heat Compensation by the Distributed Peltier Effect. In: Thermoelectrics and Their Applications (Petersburg Nuclear Physics Institute RAS, Saint-Petersburg, 2002).
 14. M.A. Korzhuev, I.V. Katin, On the Placement of Thermoelectric Generators in Automobiles, J. Electronic Materials 39 (9), 1390 – 1394 (2010).

Submitted 01.07.2011.